DOI: 10.32615/ps.2019.110 PHOTOSYNTHETICA 57 (4): 921-930, 2019

Photosynthesis response to severe water deficit in terminal stems of *Myriolimon ferulaceum*

M.À. CONESA+ and J. GALMÉS

Research Group on Plant Biology under Mediterranean Conditions, Universitat de les Illes Balears-INAGEA, Ctra. Valldemossa km. 7.5, 07122 Palma, Balearic Islands

Abstract

Myriolimon ferulaceum is a leafless species and close relative to *Limonium* inhabiting the same harsh environments in the rocky coast and salt marshes, with discontinuous distribution in western and central coast of the Mediterranean Basin and southern Iberian Peninsula. In order to test for the drought adaptive importance of photosynthesis in stems, and to decipher advantages and drawbacks of stem *vs*. leaf photosynthesis under drought conditions, *M. ferulaceum* was grown under the well-watered and severe water deficit conditions used in previous experiments with *Limonium*. Growth, stem anatomy, photosynthesis and gas exchange, and Rubisco-related traits were measured. Growth capacity in *M. ferulaceum* was higher than that of many *Limonium* under well-watered conditions, where limitations to photosynthesis were mostly biochemical. However, severe water deficit conditions had a higher impact in the leafless species, where the main photosynthesis limitation was stomatal conductance. High intrinsic water-use efficiency under well-watered conditions and high mesophyll conductance to stomatal conductance ratio under severe water deficit conditions were the main drivers of growth capacity in *M. ferulaceum*.

Additional key words: biomass; limitation analysis; *rbc*L; Rubisco kinetics; water consumption; water stress.

Introduction

Drought stress, frequently associated with high temperature and radiation, is the most important constraint to plant survival and consequently one of the main drivers of plant adaptation to the environment (Chaves *et al.* 2003, 2009). Diverse strategies to overcome drought stress have been described across species, environments, and growth forms (*e.g*. Ludlow 1989, Chaves *et al.* 2002, Lawlor and Cornic 2002, Munns, 2002, Bréda *et al.* 2006, McDowell *et al.* 2008, Nardini *et al.* 2014). Although the leaf is the main photosynthetic organ in plants, some C_3 species from arid and semiarid habitats cope with drought through different degrees of deciduousness (*e.g*. Nilsen and Sharifi 1997, Galmés *et al.* 2005, Correia and Ascensão 2017). In such cases, the photosynthesis (P_N) of green stems has an important role in plant survivorship (Nilsen 1995, Aschan and Pfanz 2003, Ávila *et al.* 2014).

Two photosynthetic syndromes have been proposed in green stems of nonsucculent plants, namely, stem net P_N and stem recycling P_N. The former occurs in stems with high stomata densities. The latter includes the cortical P_N in stems with poor or no stomata, and is also expected to occur in plants with stem net P_N (Ávila *et al.* 2014). Recycling P_N involves a large proportion of refixation of the respired CO_2. Depending on the species, it can be an important part of the overall plant carbon economy, although leaf P_N usually constitutes the main bulk. The stem net P_N is frequent in leafless desert and Mediterranean species in which the stems are the main photosynthetic organs substituting the leaf function (reviewed in Ávila *et al*. 2014, Vandegehuchte *et al.* 2015). Moreover, the stem stomatal conductance (g_s) is proportionally lower than that of the leaf (Osmond *et al.* 1987, Comstock and Ehleringer

Received 7 January 2019, *accepted* 10 July 2019.
+Corresponding author; phone: +34971171340, fax: +34971173168, e-mail: ma.conesa@uib.es
Abbreviations: B_T – total plant biomass; C_c – chloroplastic CO_2 concentration; Ep – epidermis area; ETR – electron transport rate; g_m – mesophyll conductance; g_s – stomatal conductance; g_{tot} – total leaf conductance to CO_2; J_{max} – maximum electron transport rate; K_c, K_o – Michaelis-Menten constants for CO_2 and for O_2; k^c_{cat}, k^o_{cat} – maximum rate of carboxylation and oxygenation; l_b – biochemical limitation; l_m – mesophyll limitation; l_s – stomatal limitation; Mes^{air}, Mes^{cell}, Mes^{total} – area of mesophyll airspaces, cells, and total, respectively; P_g – CO_2 assimilation rate per unit leaf area; P_N – net CO_2 assimilation rate per unit leaf area; R/S – root/shoot ratio; *rbc*L – Rubisco large subunit gene; RWC – relative water content; Scl – sclereids area; $S_{c/o}$ – Rubisco specificity factor for CO_2/O_2; Vas – vascular tissue area; V_{cmax} – maximum velocity of carboxylation; WC – water consumption; WD – severe water deficit treatment; WUE_b – whole plant water-use efficiency; WUE_i – intrinsic water-use efficiency; WW – well-watered treatment; Φ_{CO2} – quantum yield of CO_2; Φ_{PSII} – quantum yield of PSII.
Acknowledgements: This research was supported by the project AGL2009-07999 (Plan Nacional, Spain) awarded to JG. The authors thank Arantzazu Molins and Marcel Font for Rubisco kinetics and specificity factor measurement, respectively, and Miquel Truyols and collaborators of the UIB Experimental Field and Greenhouses (UIB Grant 15/2015) for their support. *M. ferulaceum* field pictures courtesy of Pere Fraga Arguimbau.

1988, Nilsen and Bao 1990, Tinoco-Ojanguren 2008) resulting in higher intrinsic water-use efficiency (WUE_i, as P_N/g_s) for the stem as compared to the leaf (Santiago *et al.* 2016). As compared to leaves, it has been suggested that the adaptive importance of green stems is higher in minimizing carbon loss through respiration rather than minimizing water loss (Berveiller *et al.* 2007, Ávila *et al.* 2014).

The Balearic species of *Limonium* inhabit harsh environments in saline soils in the rocky coast and marshes of the archipelago, where drought and salinity limit survivorship of most species. Due to the low plant occurrence, *Limonium* species are highly exposed to insolation and abrasion of the saline winds from the sea. Previous studies demonstrated important adaptations allowing to withstand severe drought conditions (Galmés *et al*. 2007a,b, 2017; Conesa *et al*. 2019). There is a large diversity in leaf size among species, and those with larger leaves have a higher growth capacity and higher water-use efficiency (Conesa *et al.* 2019). To further study the importance of leaves in the adaptation to the harsh environment of *Limonium*, it would be ideal to compare leaved and leafless *Limonium* species inhabiting the same environment. However, there are no leafless *Limonium* species in the western Mediterranean.

Myriolimon ferulaceum is a leafless species that inhabits rocky coast and marsh habitats in the Balearic Islands. This species was included within the genus *Limonium* (*i.e. L. ferulaceum*) until recently, when it was placed within a new genus based on discordant morphology, karyology, and phytochemistry (Lledó *et al.* 2003, 2005). As compared to *Limonium* plant habit, consisting in a dense and foliose subshrub cushion with seasonal reproductive branches, *M. ferulaceum* has numerous prostrate to ascendant, articulate stems up to 65 cm long, densely branched in the upper third (Erben 1993, Fig. 1S), that are maintained all year round constituting the body of the plant. Consequently, photosynthesis and gas exchange in this C_3 species is performed by stems, which have many stomata (Fig. 2S).

Given the importance of a leaf size in the response to harsh conditions previously reported in *Limonium* and its coordination with Rubisco kinetics (Galmés *et al.* 2014, 2017; Conesa *et al.* 2019), in this study we aimed to understand how the leafless strategy in the close relative *M. ferulaceum* can be also relevant under the same harsh conditions. To do so, we performed an experiment growing *M. ferulaceum* plants under the same well-watered and severe water deficit conditions as in previous studies on *Limonium*, and measured growth, water consumption and water-use efficiency, photosynthesis and gas exchange, Rubisco kinetics, and stem anatomy traits. Results showed the importance of densely branched stem structures in substituting leaf function, and denoted the modifications in stem anatomy allowing to withstand stressful conditions.

Materials and methods

Plant growth, water treatments, water consumption, and climatic conditions: Seeds from *Myriolimon ferulaceum* (L.) Lledó, Erben & M.B. Crespo were collected from natural populations in Minorca and germinated. Afterwards, ten plants were grown outdoors at the University of the Balearic Islands, individually in 3-L pots filled with a 4:1 (v/v) mixture of peat-based horticultural substrate (*Prohumin-Potting Soil Klasmann-Deilmann*, *Projar SA*, Valencia, Spain) and perlite (granulometry A13, *Projar SA*). All pots were filled to reach the same mass. Five more pots were prepared and used to calculate maximum soil water content. To do so, pots were irrigated at full capacity and left to drain plastic covered for 12 h into a room at 20°C, and weighed. The soil water content at full capacity was obtained by subtracting to the latter mass the masses of the empty pot and the dry soil. The dry mass of the soil was obtained after drying it to constant mass in trays in an air-forced oven at 70°C. Values used for calculations were the average of the five pots. The pot water content at full capacity was 2,251 g. During the experiment, the mass of the dry soil and the empty pot was used to calculate the amount of water in any pot at any moment.

Plants were initially fertilized with slow-release fertilizer and, once a week, irrigation was performed with 50% Hoagland's solution instead of water, to prevent nutrient deficiencies. After germination, irrigation was supplied at the field capacity during the spring season (15 March to 28 June) to ensure a correct plant establishment and a minimum plant size. During the summer season (29 June to 13 September), five plants were still maintained at field capacity (WW treatment), and in the remaining five, irrigation was gradually reduced during two weeks to reach a pot water content close to 45% of field capacity, and maintained below this level during the entire experiment (WD treatment). To do so, pots of both treatments were weighted and lost water replaced every 2–3 d. During the months with water treatments established, the pot water content ranged from 73% (just before irrigation; 1,643 g water in pot soil) to 100% (just after irrigation; 2,251 g water in pot soil) in WW, and from 30% (just before irrigation; 675 g water in pot soil) to 45% (just after irrigation; 1,013 g water in pot soil) in WD (Fig. 3S). Water consumption per plant (WC) corresponds to the sum of all the masses of replaced water during the three months with water treatments established.

Climatic conditions during the experiment were those typical of Mediterranean summer, with average daily temperature varying (minimum–maximum) during the experiment between 23.6–30.6°C in July, 21.6–27.2°C in August, and 17.6–23.4°C in September; daily sum of PAR ranging 6,790–15,681 μmol(photon) m^{-2} s^{-1} in July, 6,500–14,615 μmol(photon) m^{-2} s^{-1} in August, and 3,241–11,905 μmol(photon) m^{-2} s^{-1} in September; and average air relative humidity ranging 36–65% in July, 45–74% in August, and 48–83% in September.

Growth and plant water-use efficiency measurements: At the end of the experiment, 183 d after germination and after 77 d with water treatments established, all plants were cut separating stems and roots. The root ball was submerged in water overnight to ease soil separation from the roots, and gentle combed under water tab pressure. Stem and root fractions were placed in different paper envelopes and dried to constant mass in an air-forced oven

at 70°C to obtain the total plant biomass (B_T). Since the leafless plant habit of *M. ferulaceum*, the ratio between root and stem biomass corresponds to the root/shoot ratio (R/S). The water-use efficiency at the whole plant level (WUE_b) was calculated as the ratio between B_T and WC.

Stem relative water content (RWC) at mid-morning was determined as in Galmés *et al.* (2007a), at the same day as photosynthesis measurements and on the same or similar terminal stems used for gas exchange and chlorophyll (Chl) fluorescence. Five replicates per treatment were obtained from different individuals.

Stem gas exchange and Chl *a* fluorescence were measured simultaneously with an open infrared gas-exchange analyzer system equipped with a 2-cm^2 leaf chamber with a built-in fluorometer (*Li-6400-40*, *Li-Cor Inc.*, USA). Measurements were performed from 9:00 to 12:00 h during August, *i.e.* two months after the onset of the drought treatment, on intact terminal stems of five individuals; clamped terminal stems were completely developed under treatment.

Gas flow was set at 250 μmol mol^{-1} and environmental conditions in the leaf chamber consisted of a PPFD of 1,500 μmol(photon) m^{-2} s^{-1} (with 10% blue light), a vapor pressure deficit of 1.2–2.5 kPa, and a leaf temperature of 25°C. After inducing steady-state photosynthesis for at least 30 min at an ambient CO_2 concentration (C_a) of 400 μmol mol^{-1}(air), the photosynthesis response to varying substomatal CO_2 concentration (C_i) was measured as explained in Galmés *et al.* (2007b). Net photosynthesis response curves to varying substomatal CO_2 concentration (P_N-C_i) consisted of 12 measurements per curve, and five P_N-C_i were performed per treatment on different individuals. After gas-exchange measurements had been taken, the stems were sectioned and the projected area was measured by scanning it with a standard flat-bed scanner (*Epson Stylus CX3600*, *Seiko Epson Corp*., Japan), and measuring the green area on the scanned image with *Image J* (Ambràmoff *et al.* 2004). Total stem surface area was determined by multiplying the projected area by π (3.14) and divided by 2. Corrections for the leakage of CO_2 into and out of the leaf chamber of the *Li-6400-40* have been applied to all gas-exchange data, as described by Flexas *et al.* (2007).

Simultaneous measurements of Chl *a* fluorescence were made at each C_a of the P_N-C_i curve. The fluorometer was set to multiphase pulse with target intensity = 10 and ramp depth = 40%. The quantum efficiency of the PSII-driven electron transport was determined using the equation $\Phi_{PSII} = (F_m' - F_s)/F_m'$, where F_s is the steady-state fluorescence in the light [PPFD of 1,500 μmol(photon) m^{-2} s^{-1}] and F_m' the maximum fluorescence obtained with a light-saturating pulse [8,500 μmol(photon) m^{-2} s^{-1}]. As Φ_{PSII} represents the number of electrons transferred per photon absorbed by PSII, the rate of electron transport (J) can be calculated as: $J = \Phi_{PSII} \times PPFD \times \alpha \times \beta$, where α is the leaf absorbance and β is the distribution of absorbed energy between the two photosystems. The product $\alpha \times \beta$ was determined from the relationship between Φ_{PSII} and Φ_{CO2} obtained by varying C_a under nonphotorespiratory conditions in a nitrogen atmosphere containing less than 2% (v/v) O_2 (Martins *et al.* 2013). Values of $\alpha \times \beta$ averaged 0.34 with insignificant differences between treatments.

From combined gas-exchange and Chl *a* fluorescence measurements, mesophyll conductance to CO_2 (g_m) was estimated at each C_i according to Harley *et al.* (1992) as: $g_m = P_N/\{C_i - \Gamma^*[J + 8(P_N + R_D)]/[(J - 4(P_N + R_D)]\}$. Half of the rate of mitochondrial respiration in the darkness (R_D) was used here as a proxy for the rate of mitochondrial respiration in the light (R_L). R_D was measured at predawn (from 4:00 to 6:00 h) using the *Li-6400-40*. Measuring conditions in the leaf cuvette were: C_a of 400 μmol mol^{-1}(air), leaf temperature of 25°C, and vapor pressure deficit of 1.0–1.5 kPa. The chloroplast CO_2 compensation point (Γ*) was calculated from the *in vitro* Rubisco specificity factor ($S_{c/o}$) value at 25°C (obtained as indicated below) and the ambient oxygen concentration (O_A; 210,000 μmol mol^{-1}) as: $\Gamma^* = 0.5\ O_A/S_{c/o}$.

P_N-C_i curves were transformed into P_N *vs*. chloroplastic CO_2 concentration (C_c) curves using the estimated values of g_m at each C_i. From P_N-C_c curves, the maximum velocity of carboxylation (V_{cmax}) and the maximum capacity for electron transport rate (J_{max}) were calculated as in Bernacchi *et al.* (2002), but using the values for the kinetic parameters of Rubisco for *M. ferulaceum*, obtained as indicated below. The Farquhar, von Caemmerer, and Berry model (Farquhar *et al*. 1980) was fitted to the data by applying iterative curve-fitting (minimum least square difference) using *Microsoft Excel Solver* tool.

The *in vivo* photosynthetic carboxylation efficiency was inferred from the P_g/C_c ratio, being P_g the gross CO_2 assimilation rate, calculated as the sum of P_N and R_L.

Analysis of quantitative limitations of photosynthetic CO_2 assimilation: The quantitative limitation analysis of Grassi and Magnani (2005), as applied in Tomàs *et al.* (2013), was used to separate the controls on P_N resulting from limited stomatal conductance (l_s), mesophyll diffusion (l_m), and photosynthetic capacity (l_b) under WW and WD. The limitations of the different components, l_s, l_m, and l_b ($l_s + l_m + l_b = 1$) were calculated as: $l_s = [(g_{tot}/g_s)(\delta P_N/\delta C_c)]/[g_{tot} + (\delta P_N/\delta C_c)]$; $l_m = [(g_{tot}/g_m)(\delta P_N/\delta C_c)]/[g_{tot} + (\delta P_N/\delta C_c)]$; $l_b = g_{tot}/[g_{tot} + (\delta P_N/\delta C_c)]$; where g_s is the stomatal conductance to CO_2, g_m is the mesophyll conductance according to Harley *et al.* (1992), and g_{tot} is the total conductance to CO_2 from ambient air to chloroplasts. The g_{tot} was obtained as the sum of mesophyll and stomatal conductance to CO_2 considering that both are in series ($1/g_{tot} = 1/g_s + 1/g_m$). Five curves were used per treatment, and average estimates of the limitations were calculated per treatment.

Anatomical measurements of photosynthetic stems: From stems previously used in gas-exchange measurements, 8–12 fragments of *ca*. 2–3 mm were cut and immediately vacuum fixed in a phosphate buffer (0.1 M at pH 7.2, 4% glutaraldehyde and 2% paraformaldehyde), during 48 h. Afterwards, samples were washed tree times with 0.01 M PBS at pH 7.4 for 15 min, and stained/fixed with OsO_4 in 0.01 M PBS at pH 7.4 for 2 h at 4°C. A further

wash with PBS at pH 7.4 for 15 min was made, previous to dehydration with an increasing gradient of ethanol at room temperature (50, 70, 95, and 100%; for a minimum 30 min each). Dehydrated fragments were included in *Spurr*'s resin following fabricant prescription (http://www.emsdiasum.com/microscopy/technical/datasheet/14300.aspx). Semi-thin cross sections of 1 mm wide were performed using a diamond blade (*DIATOME Histo 45°*) with an ultramicrotome (*Ultratome Nova, LKB*, Bromma), stained with toluidine blue and mounted on microscope slides. Images were taken at 200 × magnification with the optic microscope *Olympus Provis AX70* equipped with an *Olympus Camedia C-2000 Z* camera (*Olympus Optical Co., Ltd.*, Tokyo, Japan).

Anatomical measurements were performed in three different plants per water treatment with *Image J* (Ambràmoff *et al.* 2004), dividing each section in four equal portions (*i.e.* ¼ portions) that were analyzed separately, resulting in $n = 12$ per plant for area measurements, namely, mesophyll airspaces (Mes^{air}), mesophyll cells (Mes^{cell}), sclereids (Scl), and vascular tissue (Vas); whereas total mesophyll area (Mes^{total}) was the sum of Mes^{air} and Mes^{cell}. To perform area measurements, images were previously modified with *Adobe Photoshop CS5* (*v. 12.1*, *Adobe*, San José, CA, USA) as in Fig. 1*A*, allowing a precise selection and separation of the different parts analyzed. Linear measurements included maximum stem diameter of the cross section and epidermis thickness (Ep), the latter being measured in four equidistant points for each ¼ portion, considering their average as the single value per ¼ portion.

Rubisco catalytic characterization: Rates of Rubisco $^{14}CO_2$-fixation using fresh leaf protein extract were measured in 7-mL septum-capped scintillation vials, containing reaction buffer (yielding final concentrations of 100 mM Bicine-NaOH, pH 8.0, 20 mM $MgCl_2$, 0.4 mM RuBP, and about 100 W-A units of carbonic anhydrase) and one of nine different concentrations of CO_2 (0 to 80 μM, each with a specific radioactivity of 3.7 × 1,010 Bq mol^{-1}), each at two concentrations of O_2 [0 and 21% (v/v)], as described previously (Galmés *et al.* 2014). Assays (1.0 mL of the total volume) were started by the addition of activated plant extract, and the maximum velocity for carboxylase activity (V_{cmax}), together with the Michaelis-Menten constant (K_m) for CO_2 (K_c) determined from the fitted data. The K_m for the oxygenase activity was calculated from the relationship $K_{c,(21\%O2)} = K_{c,(0\%O2)} \cdot (1 + [O_2]/K_o)$. The $[O_2]$ was assumed to be 265 μM, but corrected for partial pressure by taking account of the atmospheric pressure and water saturated vapor pressure. Replicate measurements ($n = 3$) were made using protein preparations from four different stems of different individuals grown under WW conditions. For each sample, the maximum rate of carboxylation (k^c_{cat}) was extrapolated from the corresponding V_{max} value after allowance was made for the Rubisco active site concentration, as determined by [^{14}C]CPBP binding (Yokota and Canvin 1985). Rubisco CO_2/O_2 specificity ($S_{c/o}$) was measured as described (Galmés *et al.* 2005) using enzyme purified by PEG precipitation and ion exchange chromatography, and the values given for each species were the mean of five to ten repeated determinations. The maximum rate of oxygenation (k^o_{cat}) was calculated using the equation $S_{c/o} = (k^c_{cat}/K_c)/(k^o_{cat}/K_o)$. All kinetic measurements were performed at 25°C.

The concentration of active Rubisco sites was calculated dividing the *in vivo* V_{cmax} by the *in vitro* k^c_{cat} measured for each species.

Statistical analysis: One-way analysis of variance (*ANOVA*) was performed to reveal the differences between treatments in the studied parameters. The univariate general linear model for unbalanced data (Proc. GLM) was applied, with type III sum of squares, and significant differences were revealed by *Duncan*'s *post-hoc* tests (at $P<0.05$) using *IBM SPSS Statistics 20* software package (*SPSS Inc.*, Chicago, IL, USA). The relationships among the parameters were tested with the square of the correlation coefficient observed for linear regressions using the tool implemented in *SigmaPlot 11.0* (*Sigma*, St Louis, MO, USA). All statistical tests were considered significant at $P<0.05$.

Results

Growth and water consumption: As compared to well-watered conditions (WW), long-term exposure to severe water deficit conditions (WD) had a dramatic effect on total plant biomass (B_T) in *M. ferulaceum*, with more than 4-fold reduction (Table 1). The water consumption during the water treatments application (WC) was 6-fold lower under WD and, thus, proportionally higher than B_T reduction. Consequently, water-use efficiency at the whole plant level (WUE_b, as B_T/WC) might be on average higher under WD than under WW conditions, but differences between treatments were insignificant (Table 1). Plants under WD had 2-fold higher root/shoot ratio (R/S) than that of WW plants and, thus, this species responded to severe water deficit by a notorious increase in the proportion of root biomass (Table 1). The relative water content in the stems (RWC) was also significantly affected by the water deficit, with a 12% lower value under WD (Table 1).

Stem anatomy: Stems under WD were significantly thinner than that under WW, with the stem section and

Table 1. Growth and water-use parameters for *Myriolimon ferulaceum* grown under field capacity (WW) and severe water deficit (WD). B_T – total plant biomass; R/S – root to shoot ratio; WC – water consumed during the period between 29 June and 13 September; WUE_b – water-use efficiency at the whole plant level; RWC – stem relative water content. *ANOVA P*-value is indicated for each parameter. Data are means ± SE ($n = 5$).

Parameter	WW	WD	*P*-value
B_T [g]	11.5 ± 0.7	2.7 ± 0.4	<0.001
R/S	0.53 ± 0.06	1.07 ± 0.21	<0.001
WC [L plant^{-1}]	10.6 ± 1.3	1.8 ± 0.1	<0.001
WUE_b [g L^{-1}]	0.80 ± 0.10	0.71 ± 0.08	0.243
RWC [%]	77 ± 1	65 ± 1	<0.001

the stem diameter being 20 and 10% smaller, respectively (Fig. 1*A*, Table 2). Considering the components in the stem section, all were reduced except the area of the total mesophyll (Mes^{total}) and the area of the mesophyll airspaces (Mes^{air}). Therefore, the latter two components proportionally increased under WD to remain similar between treatments despite of the reduction on the total stem thickness under WD. This proportional increase in Mes^{total} and Mes^{air} was at expenses of a proportionally higher reduction in the mesophyll cells (Mes^{cell}), sclereids (Scl), and vascular tissue (Vas), but not epidermis (Ep), which was thicker under WD (Fig. 1*B*, Table 2).

Photosynthesis and gas exchange: The WD treatment had also an important effect on the photosynthesis performance of *M. ferulaceum*, with differences between treatments in all the measured parameters (Table 3). There was a 3.6-fold lower stem P_N under WD as compared to WW, and a significant relationship was observed between P_N and B_T (R^2 = 0.76, P<0.001; data not shown). There was also a 6.3-fold lower stem g_s under WD, very similar to the 6-fold difference in WC between treatments. A significant relationship was also observed between g_s and WC (R^2 = 0.59, P<0.001; data not shown). Different from WUE_b, the intrinsic water-use efficiency (WUE_i, as P_N/g_s) was 1.7-fold higher under WD as compared to WW (Table 3).

The mesophyll conductance (g_m) was 2.3-fold lower under WD which, added up to the difference in g_s, resulted in a 4-fold lower g_{tot} under WD (Table 3). The g_m/g_s ratio increased from 1.3 under WW to 3.1 under WD (Table 3), and positively correlated with WUE_i under both treatments (WW, R^2 = 0.932; WD, R^2 = 0.887; P<0.001 in both cases) and also considering both treatments together (Fig. 2), denoting a similar scale-up of g_m/g_s and WUE_i under WD as compared to WW.

The CO_2 concentration at the chloroplast stroma (C_c) was 1.6-fold lower under WD, being responsible for the lower P_N values in this treatment (Table 3). When considering the gross photosynthesis (P_g), the photosynthetic efficiency (P_g/C_c) was 2-fold lower under WD, whereas photorespiration (considering the electron transport rate, *i.e.* ETR/P_g), was 1.6-fold higher under WD (Table 3). The maximum rate of photosynthetic electron transport (J_{max}) was also severely depressed under WD.

Rubisco-related traits and Rubisco kinetic properties: There were differences in the Rubisco active sites between treatments, being 2.1-fold lower under WD, and agreeing with the 2.1-fold lower maximum rate of Rubisco carboxylation velocity (V_{cmax}) under this treatment (Table 3).

Regarding the catalytic parameters of Rubisco from *M. ferulaceum* (Table 4), the maximum rates of carboxylation (k^c_{cat}) and oxygenation (k^o_{cat}) were 2.9 s^{-1} and 1.4 s^{-1}, respectively. The Michaelis-Menten constants affinity for CO_2 (K_c) and O_2 (K_o) were 7.4 and 466 μM, respectively, and the specificity factor ($S_{c/o}$) was 102.5 mol mol^{-1}.

The quantitative limitation analysis of photosynthetic CO_2 assimilation showed a similar importance of the three limitations under WW. Under WD, the biochemical limitation (l_b) decreased and stomatal conductance limitation (l_s) increased as compared to WW (Fig. 3). In spite of the proportional changes in the limitations components, P_N correlated with both g_{tot} and V_{cmax} (Fig. 4).

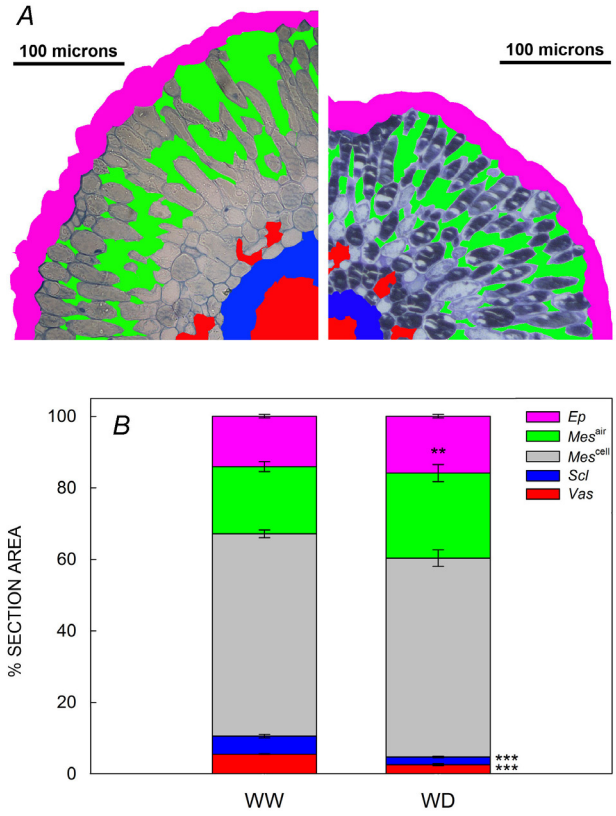

Fig. 1. Anatomical differences between the well-watered (WW) and severe water deficit (WD) treatments of *Myriolimon ferulaceum* plants. A shoot section was measured from three different plants per treatment. Each section was divided into four pieces that were measured separately, thus n = 12 for all the parameters. Thicknesses were measured in four equidistant points in each of the pieces and values were averaged to consider a single value per piece. (*A*) Piece (¼) of the section for WW (*left*) and WD (*right*), indicating the different components in colors: epidermis (Ep, *purple*), mesophyll airspaces (Mes^{air}, *green*), mesophyll cells (Mes^{cell}, *grey/uncolored*), sclereids (Scl, *blue*), and vascular tissue (Vas, *red*). (*B*) Percent of the total section for the different components. Correspondence of components and colors as in (*A*). Percent differences between treatments by one-way *ANOVA* are indicated with asterisks in the WD column ($^{***}P$<0.001, $^{**}P$<0.01, $^{*}P$<0.05).

Discussion

Leafless plant habit is frequently considered an adaptive strategy to cope with severe drought conditions (*e.g.* Nilsen and Sharifi 1997, Galmés *et al.* 2005, Correia and Ascensão 2017). However, similar to leaved species, stems in the leafless *M. ferulaceum* suffered important modifications to withstand stressful conditions. As compared to the close relative and leaved *Limonium* species, the leafless strategy in *M. ferulaceum* presented higher limitations to overcome severe water deficit.

Table 2. Anatomical differences between the well-watered (WW) and severe water deficit (WD) treatments for the whole cross section, and for epidermis (Ep), mesophyll airspaces (Mes^{air}), mesophyll cells (Mes^{cell}), sclereids (Scl), and vascular tissue (Vas) of *Myriolimon ferulaceum*. A shoot section was measured from three different plants per treatment. Values are averages with SE. Each section was divided in four pieces that were measured separately, thus $n = 12$ for all the parameters. Differences between treatments by one-way *ANOVA* are indicated (*P*-values). *See* Fig. 1 for a reference.

	WW	WD	*P*-value
Cross section area [μm²]	272,307 ± 11,037	218,874 ± 7,168	0.001
Cross section maximum diameter [μm]	633.5 ± 11.9	569.1 ± 13.5	0.002
Ep thickness	22.0 ± 0.6	24.0 ± 0.7	0.032
Mes^{total} area [μm²]	206,319 ± 11,065	181,290 ± 6,704	0.124
Mes^{air} area [μm²]	52,327 ± 5,354	55,487 ± 7,304	0.712
Mes^{cell} area [μm²]	153,992 ± 7,243	125,802 ± 4,302	0.020
Scl area [μm²]	13,135 ± 953	4,448 ± 265	<0.001
Vas area [μm²]	14,730 ± 426	5,050 ± 576	<0.001

Table 3. Average values for the main photosynthetic parameters in *Myriolimon ferulaceum* under field capacity (WW) and severe water deficit (WD) treatments. Net CO_2 assimilation rate (P_N), stomatal, mesophyll, and total leaf conductances (g_s, g_m, g_{tot}, respectively), intrinsic water-use efficiency (WUE_i), CO_2 concentration in the chloroplast (C_c), CO_2 assimilation rate (P_g), and electron transport rate (ETR) were obtained from steady state measurements at a PPFD of 1,500 μmol(photon) m^{-2} s^{-1}, with a leaf temperature of 25ºC, and a CO_2 concentration in the chamber of 400 μmol mol^{-1}. Maximum velocity of carboxylation (V_{cmax}) and maximum electron transport rate (J_{max}) were estimated from P_N-C_c curves. The active Rubisco sites were calculated dividing *in vivo* V_{cmax} by the *in vitro* maximum rate of carboxylation (k^c_{cat}). *ANOVA P*-value is indicated for each parameter. Data are means ± SE ($n = 5$). All area-based parameters were corrected to account for the semicircular surface of the stems, dividing the measured value by π/2.

Parameter	WW	WD	*P*-value
P_N [μmol m^{-2} s^{-1}]	14.1 ± 1.5	3.9 ± 0.3	<0.001
g_s [mol(H_2O) m^{-2} s^{-1}]	0.19 ± 0.03	0.03 ± 0.01	<0.001
g_m [mol m^{-2} s^{-1}]	0.14 ± 0.02	0.06 ± 0.01	0.001
g_{tot} [mol m^{-2} s^{-1}]	0.08 ± 0.01	0.02 ± 0.01	<0.001
WUE_i [μmol mol^{-1}]	78 ± 5	135 ± 5	<0.001
g_m/g_s [mol(CO_2) mol^{-1}(CO_2)]	1.3 ± 0.2	3.1 ± 0.5	0.012
C_c [μmol mol^{-1}]	151 ± 4	94 ± 6	<0.001
P_g/C_c [mol m^{-2} s^{-1}]	0.10 ± 0.01	0.05 ± 0.01	<0.001
ETR/P_g	8.1 ± 0.1	12.6 ± 0.9	0.001
V_{cmax} [μmol m^{-2} s^{-1}]	75.5 ± 7.6	35.3 ± 1.0	<0.001
J_{max} [μmol m^{-2} s^{-1}]	125.8 ± 11.9	53.1 ± 2.1	<0.001
Active Rubisco sites [μmol m^{-2}]	26.0 ± 2.6	12.2 ± 0.3	<0.001

The adaptation of *M. ferulaceum* to severe water shortage resulted in dramatic reductions of WC (6-fold) and B_T (4-fold) but with no significant differences in WUE_b (Table 1). The latter could indicate that this leafless species did not trigger mechanisms improving biomass produced per unit water consumed under harsh conditions. However, WD plants had a 2-fold higher R/S (Table 1). Proportionally larger roots as compared to shoots would allow higher soil exploration, and higher root biomass per unit stem – transpiring – biomass. A similar WUE_b between treatments achieved through a proportionally lower photosynthetic biomass indicates that morpho-physiological adaptations increasing photosynthetic efficiency took place in the WD stems.

The severe water shortage entailed a *ca*. 6-fold reduction of g_s under WD (Table 3). As a result, Rubisco had to operate at lower C_c, which imposed a limitation to maximum P_N and resulted in lower photosynthetic efficiency (P_g/C_c) (Table 3). However, WUE_i was 1.7-fold higher under WD. This, together with the 2.3-fold higher g_m and 4-fold higher g_{tot} (Table 3), and the tight control of P_N driven by g_{tot} (Fig. 4*A*), indicated that the morpho-physiological adaptations under WD improved CO_2 diffusion per unit water transpired. Changes in WUE_i were positively correlated with the g_m/g_s ratio (Fig. 2), which increased from 1.3 under WW to 3.1 under WD (Table 3). The WD stems were thinner, with a 20% reduction of the stem section area through a decrease of Scl, Vas, and Mes^{cell}, but maintaining Mes^{total} and Mes^{air} areas similar to those in WW, corresponding to a proportional increase of mesophyll airspaces under WD (Fig. 1, Table 2). Increase of airspaces is a common mechanism leading to increased g_m, because of higher access of the mesophyll cells to CO_2 (Flexas *et al.* 2013, 2016; Galmés *et al.* 2013). Also, it would be expected that thinner stems under WD might have lower WUE_i because of lower proportion of

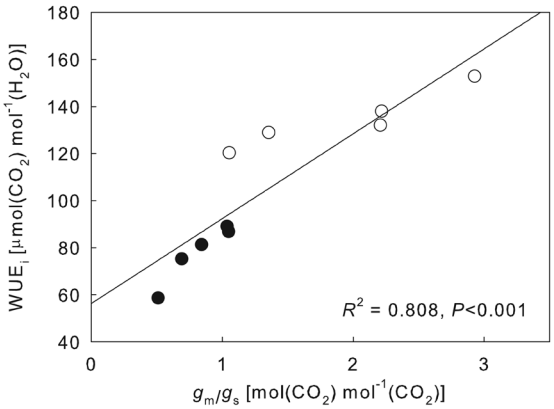

Fig. 2. The relationship between mesophyll and stomatal conductances (g_m/g_s) and the intrinsic water-use efficiency (WUE_i) of *Myriolimon ferulaceum* plants. *Filled black circles* represent well-watered (WW) plants and *empty circles* represent severe water deficit (WD) plants. *The regression line* corresponds to both treatments together. Results are similar when considering treatments separately (WW, $R^2 = 0.932$; WD, $R^2 = 0.887$; $P<0.001$ in both cases).

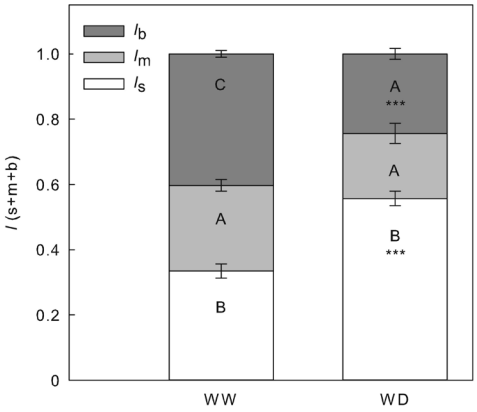

Fig. 3. Quantitative limitation analysis of photosynthetic CO_2 assimilation of *Myriolimon ferulaceum* plants under field capacity (WW) and severe water deficit (WD) treatments. The stomatal (l_s), mesophyll (l_m), and biochemical (l_b) limitations of photosynthetic assimilation are shown for each treatment. Values are means ± SE (n = 5). *Different letters* denote statistically significant differences ($P<0.05$) between limitations within each water treatment by *Tukey*'s *post-hoc* test. Asterisks in WD mean significant difference between water treatments at $^{*}P\leq0.05$, $^{**}P\leq0.01$ or $^{***}P\leq0.001$.

Table 4. Rubisco kinetic parameters at 25°C for *Myriolimon ferulaceum*. Rubisco kinetic parameters describe the Michaelis-Menten constants for CO_2 (K_c) and O_2 (K_o), maximum rate of carboxylation (k^c_{cat}) and carboxylation catalytic efficiency (k^c_{cat}/K_c), specificity factor ($S_{c/o}$), maximum rate of oxygenation (k^o_{cat}), and oxygenation catalytic efficiency (k^o_{cat}/K_o). Data are means ± SE (n = 3). The maximum rate of oxygenation (k^o_{cat}) was calculated using the equation $S_{c/o} = (k^c_{cat}/K_c)/(k^o_{cat}/K_o)$.

Parameter	Average ± SE
K_c [μM]	7.4 ± 0.2
$K_{c,air}$ [μM]	13.4 ± 1.9
K_o [μM]	377 ± 44
k^c_{cat} [s^{-1}]	2.9 ± 0.2
k^c_{cat}/K_c [s^{-1} μM^{-1}]	0.39 ± 0.04
$S_{c/o}$ [mol mol^{-1}]	102.5 ± 1.8
k^o_{cat} [s^{-1}]	1.4 ± 0.4
k^o_{cat}/K_o [s^{-1} μM^{-1}]	2.36 ± 0.71

photosynthetic mesophyll cells (*i.e.* volume-related) per unit transpiring surface (*i.e.* area-related). This can be related at least to three reasons. First, maximization of P_N *vs*. light penetration into thicker stems (Pfanz *et al.* 2002), *i.e.* thinner stems may enhance maximum P_N in most mesophyll cells. Second, the reduction in vascular tissue under WD may limit water availability for outermost cells in thicker stems. It has been demonstrated that the widely known coordination between hydraulic conductance and P_N in leaves (*e.g.* Scoffoni *et al.* 2016) also occurs in photosynthetic stems (Ávila-Lovera *et al.* 2017). Third, a reduction in sclereids under WD may limit plant ability to sustain stems and thus, forcing stems to be thinner.

Agreeing with the importance of the g_m/g_s ratio in explaining WUE_i improvement (Fig. 2), the quantitative limitation analysis of photosynthetic CO_2 assimilation (Fig. 3) showed that the main limitation under WD was stomatal conductance (l_s), with a similar importance of mesophyll diffusion (l_m) and biochemistry (l_b). On the contrary, under WW the most restricting factor was biochemistry and the least mesophyll diffusion (Fig. 3). Predominance of biochemical limitation under nonstressing conditions and stomatal limitation under drought is a common pattern in angiosperms from arid and semiarid habitats like the Mediterranean (Tomàs *et al.* 2013, Flexas *et al.* 2014, Carriquí *et al.* 2015), and particularly in the Mediterranean *Limonium* species (Galmés *et al.* 2017), which are close relatives of *M. ferulaceum* and inhabiting very similar environments.

From the three Rubisco haplotypes described in *Limonium*, the haplotype I, which is basal to the remaining two (Galmés *et al.* 2014), showed a biochemical limitation almost as high as the stomatal limitation under WD (Galmés *et al.* 2017). The derived haplotypes II and III had slower velocity (lower k^c_{cat}), higher specificity for CO_2 ($S_{c/o}$) and consequently lower P_N than that of haplotype I, which indicates that Rubisco evolution in the harsh habitats of *Limonium* favored Rubiscos with higher efficiency under low C_c (lower g_{tot}) (Galmés *et al.* 2014, 2017). As compared to *Limonium* haplotypes, *M. ferulaceum* Rubisco better resembled those of haplotypes II and III, with stomatal limitations being *ca*. 50% of the total limitations (Fig. 3; Galmés *et al.* 2017). However, the kinetics of *M. ferulaceum* Rubisco did not match with the values reported for the *Limonium* haplotypes. It resembled the haplotypes II and III in having lower K_c, K_o, and k^c_{cat}, but resembled haplotype I in having high k^o_{cat} and k^c_{cat}/K_c, and low $S_{c/o}$ and k^o_{cat}/K_o. In fact, *M. ferulaceum* Rubisco had lower $S_{c/o}$ and k^o_{cat}/K_o and higher carboxylase catalytic efficiency (k^c_{cat}/K_c) than any *Limonium* species (Table 4; Galmés *et al.* 2014).

Regarding this intermediate behavior between haplo-

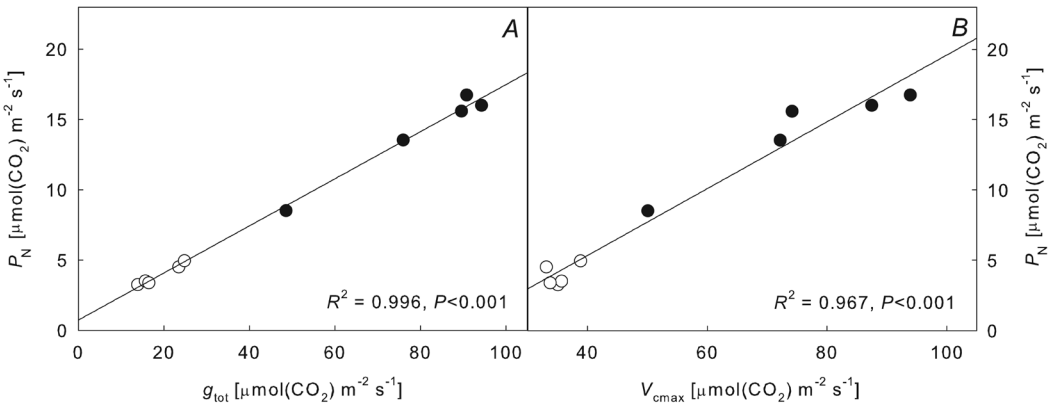

Fig. 4. The relationship between the net CO_2 assimilation rate (P_N) and the total conductance to CO_2 (g_{tot}) (*A*) and the maximum rate of Rubisco carboxylation (V_{cmax}) (*B*). *Filled black circles* represent well-watered (WW) plants and *empty circles* represent severe water deficit (WD) plants. *The regression lines* correspond to both treatments together. Considering treatments separately, (*A*) WW, R^2 = 0.978; WD, R^2 = 0.968; P<0.001 in both cases, and (*B*) WW, R^2 = 0.899, P<0.001; WD, P>0.05.

types I and II–III, there is larger number of differences between the *rbc*L amino acid sequence of *M. ferulaceum* (Genbank number: KJ608035.1) and any of the *Limonium* Rubiscos (*i.e.* 14 residues), than between *Limonium* Rubiscos (*i.e.* 6 residues) (Table 1S). *M. ferulaceum* differs from *Limonium* haplotypes I, II, and III in 9, 11, and 12 positions, respectively. Consequently, *M. ferulaceum rbc*L has higher similarity with haplotype I. In *Limonium*, changes in residues 309, 328, and 340 were related to higher specificity for CO_2 and lower carboxylation velocity in haplotypes II–III (Galmés *et al.* 2014). In *M. ferulaceum rbc*L, positions 309 and 328 are coincident with haplotype I and position 340 is coincident with haplotypes II–III (Table 1S). Nevertheless, further work is needed to ascertain an impact of these amino acid changes in the different kinetics observed among Rubiscos of *M. ferulaceum* and *Limonium*.

The P_N values of *M. ferulaceum* (Table 3) fall within the maximum stem P_N documented, ranging from 1.7 to 20.9 μmol(CO_2) m^{-2} s^{-1}, which mostly correspond to species from arid environments having also leaf photosynthesis. In such species, leaves attain most of the year-round photosynthetic function, although stem photosynthesis can be similar or exceed that of the leaf in particular cases (reviewed in Ávila *et al.* 2014).

When comparing the leafless *M. ferulaceum* with leaved *Limonium* species grown under the same conditions, not only P_N, but also g_s, g_m, P_g/C_c, V_{cmax}, J_{max}, and active Rubisco sites were lower in the former species than in most *Limonium* (Table 3; Galmés *et al.* 2017) denoting the limitations to photosynthesis and gas exchange of the stems. Under WW, B_T in *M. ferulaceum* was higher than 8 out of 13 *Limonium* species (Table 1; Conesa *et al.* 2019), indicating that the leafless plant habit is actually not detrimental when compared to leaved species. In this regard, WUE_i in *M. ferulaceum* was among the highest values in *Limonium* (Table 3; Galmés *et al.* 2017), pointing to this as one of the main factors driving higher growth capacity of *M. ferulaceum* stems as compared to many *Limonium* leaves under nonstressing conditions. One of the most relevant benefits in arid species for switching to stem photosynthesis in the toughest season is the higher WUE_i as compared to leaves, which has been related to the presence of sunken stomata, the vertical orientation of the stem diminishing photoinhibitory damage, and the lower sensitivity to environmental factors, such as drought, high temperature, low VPD, and low resources availability, among others (reviewed in Ávila *et al.* 2014, 2017; Santiago *et al.* 2016). The stem CO_2 assimilation in these species has shown to be higher in the dry than in the wet season because of seasonal acclimation to higher light and temperature (Ávila-Lovera *et al.* 2017).

Contrary to the above, *M. ferulaceum* does not have sunken stomata (Fig. 3S), and photosynthesis and growth were dramatically affected under WD (Tables 1, 3). Hence, as compared to *Limonium* and paralleling WW, under WD, *M. ferulaceum* had much lower values of most of the measured photosynthetic parameters, much higher difference between treatments than those reported for *Limonium* species (Table 3; Galmés *et al.* 2014), and lower B_T than any *Limonium* species (Conesa *et al.* 2019). Consequently, stem photosynthesis appears as a worse adaptive strategy to severe water deficit than that in the leaved *Limonium* species.

Altogether, results show that the thin and branched stems in *M. ferulaceum* cope well with the function of leaves in C_3 species under WW conditions, but have important limitations to minimize growth reduction under harsh environments, as compared to leaves in *Limonium*. The severe water deficit resulted in high decreases in growth and water consumption but also adaptations related to increased water-use efficiency, such as increased R/S, and increased mesophyll airspaces leading to increased g_m and especially the g_m/g_s ratio. There was a tight control of P_N by V_{cmax} and g_{tot}, whereas the main limitation to P_N under WW was biochemical (*i.e.* Rubisco concentration and activity) and under WD diffusive (mostly stomatal).

Given the distribution of *M. ferulaceum* in the Mediterranean Basin, with narrow and disjunct populations (Lledó *et al.* 2003), increased intensity and duration of drought periods as predicted by the climate change scenario may have a negative impact for population survivorship,

with dramatic effects on the species' distribution. Thus, despite the resilience to stress supposed to leafless species inhabiting harsh environments, *M. ferulaceum* showed less adaptability as compared to *Limonium* species, which may be considered to properly define managing strategies for conservation purposes.

References

Ambràmoff M.D., Magalhães P.J., Ram S.J.: Image processing with ImageJ. – Biophotonics Int. **11**: 36-42, 2004.

Aschan G., Pfanz H.: Non-foliar photosynthesis – a strategy of additional carbon acquisition. – Flora **198**: 81-97, 2003.

Ávila E., Herrera A., Tezara W.: Contribution of stem CO_2 fixation to whole-plant carbon balance in nonsucculent species. – Photosynthetica **52**: 3-15, 2014.

Ávila-Lovera E., Zerpa A.J., Santiago L.S.: Stem photosyntheis and hydraulics are coordinated in desert plant species. – New Phytol. **216**: 1119-1129, 2017.

Bernacchi C.J., Portis A.R., Nakano H. *et al.*: Temperature response of mesophyll conductance. Implications for the determination of Rubisco enzyme kinetics and for limitations to photosynthesis *in vivo*. – Plant Physiol. **130**: 1992-1998, 2002.

Berveiller D., Kierzkowski D., Damesin C.: Interspecific variability of stem photosynthesis among tree species. – Tree Physiol. **27**: 53-61, 2007.

Bréda N., Huc R., Granier A., Dreyer E.: Temperate forest trees and stands under severe drought: a review of ecophysiological responses, adaptation processes and long-term consequences. – Ann. For. Sci. **63**: 625-644, 2006.

Carriquí M., Cabrera H.M., Conesa M.À. *et al.*: Diffusional limitations explain the lower photosynthetic capacity of ferns as compared with angiosperms in a common garden study. – Plant Cell Environ. **38**: 448-460, 2015.

Chaves M.M., Flexas J., Pinheiro C.: Photosynthesis under drought and salt stress: regulation mechanisms from whole plant to cell. – Ann. Bot.-London **103**: 551-560, 2009.

Chaves M.M., Maroco J.P., Pereira J.S.: Understanding plant responses to drought – from genes to the whole plant. – Funct. Plant Biol. **30**: 239-264, 2003.

Chaves, M.M., Pereira J.S., Maroco J. *et al*.: How plants cope with water stress in the field. Photosynthesis and growth. – Ann. Bot.-London **89**: 907-916, 2002.

Comstock J.P., Ehleringer J.R.: Contrasting photosynthetic behavior in leaves and twigs of *Hymenoclea salsola*, a green-twigged warm desert shrub. – Am. J. Bot. **75**: 1360-1370, 1988.

Conesa M.À., Mus M., Galmés J.: Leaf size as a key determinant of contrasting growth patterns in closely related *Limonium* (Plumbaginaceae) species under well-watered and severe water deficit conditions. – J. Plant Physiol. **240**: 152984, 2019.

Correia O., Ascensão L.: Summer semi-deciduous species of the Mediterranean landscape: A winning strategy of *Cistus* species to face the predicted changes of the Mediterranean climate. – In: Ansari A.A., Gill S.S., Abbas Z.K., Naeem M. (ed.): Plant Biodiversity: Monitoring, Assessment and Conservation. Pp. 195-217. CABI International, *Wallingford* 2017.

Erben M.: *Limonium*. – In: Castroviejo S., Aedo C., Cirujano S. *et al*. (ed.): Flora Iberica. Vol. 3. Pp. 2-143. Real Jardín Botánico-C.S.I.C., Madrid 1993.

Farquhar G., von Caemmerer S., Berry J.A.: A biochemical-model of photosynthetic CO_2 assimilation in leaves of C_3 species. – Planta **149**: 78-90, 1980.

Flexas J., Díaz-Espejo A., Berry J.A. *et al*.: Analysis of leakage in IRGA's leaf chambers of open gas photosynthesis parameterization. – J. Exp. Bot. **58**: 1533-1543, 2007.

Flexas J., Díaz-Espejo A., Conesa M.À. *et al*.: Mesophyll conductance to CO_2 and Rubisco as targets for improving intrinsic water use efficiency in C_3 plants. – Plant Cell Environ. **39**: 965-982, 2016.

Flexas J., Díaz-Espejo A., Gago J. *et al*.: Photosynthetic limitations in Mediterranean plants: a review. – Environ. Exp. Bot. **103**: 12-23, 2014.

Flexas J., Niinemets U., Gallé A. *et al*.: Diffusional conductances to CO_2 as a target for increasing photosynthetic water-use efficiency. – Photosynth. Res. **117**: 45-59, 2013.

Galmés J., Andralojc P.J., Kapralov M.V. *et al*.: Environmentally driven evolution of Rubisco and improved photosynthesis and growth within the C_3 genus *Limonium* (Plumbaginaceae). – New Phytol. **203**: 989-999, 2014.

Galmés J., Flexas J., Keys A.J. *et al*.: Rubisco specificity factor tends to be larger in plant species from drier habitats and in species with persistent leaves. – Plant Cell Environ. **28**: 571-579, 2005.

Galmés J., Flexas J., Savé R., Medrano H.: Water relations and stomatal characteristics of Mediterranean plants with different growth forms and leaf habits: responses to water stress and recovery. – Plant Soil **290**: 139-155, 2007a.

Galmés J., Medrano H., Flexas J.: Photosynthetic limitations in response to water stress and recovery in Mediterranean plants with different growth forms. – New Phytol. **175**: 81-93, 2007b.

Galmés J., Molins A., Flexas J., Conesa M.À.: Coordination between leaf CO_2 diffusion and Rubisco properties allow maximizing photosynthetic efficiency in *Limonium* species. – Plant Cell Environ. **40**: 2081-2094, 2017.

Galmés J., Perdomo J.A., Flexas J., Whitney S.M.: Photosynthetic characterization of Rubisco transplantomic lines reveals alterations on photochemistry and mesophyll conductance. – Photosynth. Res. **115**: 153-166, 2013.

Grassi G., Magnani F.: Stomatal, mesophyll conductance and biochemical limitations to photosynthesis as affected by drought and leaf ontogeny in ash and oak trees. – Plant Cell Environ. **28**: 834-849, 2005.

Harley P.C., Loreto F., Di Marco G., Sharkey T.D.: Theoretical considerations when estimating the mesophyll conductance to CO_2 flux by the analysis of the response of photosynthesis to CO_2. – Plant Physiol. **98**: 1429-1436, 1992.

Lawlor D.W., Cornic G.: Photosynthetic carbon assimilation and associated metabolism in relation to water deficits in higher plants. – Plant Cell Environ. **25**: 275-294, 2002.

Lledó M.D., Erben M., Crespo M.B.: *Myriolepis*, a new genus segregated from *Limonium* (Plumbaginaceae). – Taxon **52**: 67-73, 2003.

Lledó M.D., Erben M., Crespo M.B.: *Myriolimon*, a new name for a recently published *Myriolepis* (Plumbaginaceae). – Taxon **54**: 811-812, 2005.

Ludlow M.M.: Strategies of response to water stress. – In: Kreeb K.H., Richter H., Hinckley T.M. (ed.): Structural and Functional Responses to Environmental Stresses. Pp. 269-281. SPB Academic Publishing, The Hague 1989.

Martins S.C.V., Galmés J., Molins A., DaMatta F.M.: Improving the estimation of mesophyll conductance to CO_2: on the role of electron transport rate correction and respiration. – J. Exp. Bot. **64**: 3285-3298, 2013.

McDowell N., Pockman W.T., Allen C.D. *et al*.: Mechanisms of plant survival and mortality during drought: why do some plants survive while others succumb to drought? – New Phytol. **178**: 719-739, 2008.

Munns R.: Comparative physiology of salt and water stress. – Plant Cell Environ. **25**: 239-250, 2002.

Nardini A., Lo Gullo M.A., Trifilò P., Salleo S.: The challenge of the Mediterranean climate to plant hydraulics: Responses and adaptations. – Environ. Exp. Bot. **103**: 68-79, 2014.

Nilsen E.T.: Stem photosynthesis: extent, patterns, and role in plant carbon economy. – In: Gartner B.L. (ed.): Plant Stems. Pp. 223-240. Academic Press, San Diego 1995.

Nilsen E.T., Bao Y.: The influence of water stress on stem and leaf photosynthesis in *Glycine max* and *Sparteum junceum* (Leguminosae). – Amer. J. Bot. **77**: 1007–1015, 1990.

Nilsen E.T., Sharifi M.: Carbon isotopic composition of legumes with photosynthetic stems from mediterranean and desert habitats. – Am. J. Bot. **84**: 1707-1713, 1997.

Osmond C.B., Smith S.D., Gui-Ying B., Sharkey T.D.: Stem photosynthesis in a desert ephemeral, *Eriogonum inflatum*. Characterization of leaf and stem CO_2 fixation and H_2O vapor exchange under controlled conditions. – Oecologia **72**: 542-549, 1987.

Pfanz H., Aschan G., Langenfeld-Heyser R. *et al*.: Ecology and ecophysiology of tree stems: corticular and wood photosynthesis. – Naturwissenschaften **89**: 147-162, 2002.

Santiago L.S., Bonal D., De Guzman M.E., Ávila-Lovera E.: Drought survival strategies of tropical trees. – In: Goldstein G., Santiago L.S. (ed.): Tropical Tree Physiology. Pp. 243-258. Springer International Publishing, Basel 2016.

Scoffoni C., Chatelet D.S., Pasquet-Kok J. *et al*.: Hydraulic basis for the evolution of photosynthetic productivity. – Nat. Plants **2**: 16072, 2016.

Tinoco-Ojanguren C.: Diurnal and seasonal patterns of gas exchange and carbon gain contribution of leaves and stems of *Justicia californica* in the Sonoran Desert. – J. Arid Environ. **72**: 127-140, 2008.

Tomàs M., Flexas J., Copolovici L. *et al*.: Importance of leaf anatomy in determining mesophyll diffusion conductance to CO_2 across species: quantitative limitations and scaling up by models. – J. Exp. Bot. **64**: 2269-2281, 2013.

Vandegehuchte M.W., Bloemen J., Vergeynst L.L., Steppe K.: Woody tissue photosynthesis in trees: salve on the wounds of drought? – New Phytol. **208**: 998-1002, 2015.

Yokota A., Canvin D.T.: Ribulose bisphosphate carboxylase/oxygenase content determined with [^{14}C]carboxypentitol bisphosphate in plants and algae. – Plant Physiol. **77**: 735-739, 1985.